Structural Chemistry
https://doi.org/10.1007/s11224-025-02483-w

RESEARCH

First-principles study of dynamic symmetry in acrylic acid

Luca Sironi[1] · Giovanni Macetti[1] · Margherita Vacchini[1] · Leonardo Lo Presti[1]

Received: 5 January 2025 / Accepted: 5 March 2025
© The Author(s) 2025

Abstract
Average crystallographic structures may disguise more complex packing modes, such as commensurate modulations that originate from coherent librational distortions of the lattice. These can be easily overlooked, with striking implications on the understanding of intermolecular interactions, provided that the crystal is described in terms of colorless symmetries. As shown in the 1970s by Kołakowski, lattice modulations with strong librational components can be understood in terms of colored group operations applied to pseudovector quantities, like rotation momenta. Here, we employ Kołakowski's concepts of dynamic symmetry to computationally predict modulated distortions in crystalline acrylic acid. We show that periodic lattice distortions may indeed originate from a low-frequency phonon instability at the Γ point of the first Brillouin zone. The packing of the corresponding molecular libration momenta is analogue to an antiferromagnetic ordering in the $I_c bam$ Shubnikov group, which can be also described as a commensurate modulation emerging from (3 + 1)D *Imcb*(00γ)0*s*0 superspace structure with $\gamma = 1$. In the reciprocal lattice, the distortions produce exceptions to the systematic extinction rules, due to the scattering at commensurate Bragg points that derive from the reduced colorless symmetry. This evidence offers an easy strategy to look for such phenomena in X-ray experiments, also taking advantage of the sensitivity of modern area detectors. Implications on the onset of phase transitions in organic crystals are also discussed.

Keywords Molecular dynamics · Acrylic acid · Lattice distortions · Dynamic symmetry · Colored symmetry · Superspace groups

Introduction

Crystallographers are accustomed to thinking in terms of mean static structures, as derived from the analysis of the corresponding X-ray diffraction patterns. Accordingly, crystal packing is described by the symmetry operations of the 230 colorless space groups [1], applied to least-squares averaged atomic coordinates. The success of this model over the last century is undeniable, as testified by the ever-growing flourishing of huge and reliable crystallographic databases [2, 3] However, dynamic effects like the reorientation of terminal groups[4, 5], or even of whole molecules [6, 7] are crucial to explain mechanical and thermal properties of molecular crystals, including the onset of phase transitions [8]. Moreover, low-frequency lattice libration modes [9] provide significant contributions to the atomic displacement amplitudes [10, 11] and may result in a significant deviation from the average crystallographic symmetry. Recently, one of us studied 1-methyluracil at 23 K (CCDC METURA15) [12]. It crystallizes in *Ibam*, with molecules constrained to lie in the mirror plane and packed into perfectly flat parallel sheets along the *c* axis. No evidence of disorder was detected in the X-ray dataset, which consisted of Bragg effects measured with a point detector; nevertheless, unexplained Fourier residuals, up to + 0.4–0.5 e·Å^{-3}, were found close to methyl and oxygen groups. These peaks survived the refinement of multipole charge density parameters and anharmonic Gram–Charlier tensor components, indicating that the model lacked some kind of structural information. Classical molecular dynamics (MD) simulations found that the structure is

✉ Giovanni Macetti
giovanni.macetti@unimi.it

✉ Leonardo Lo Presti
leonardo.lopresti@unimi.it

Luca Sironi
luca.sironi1@unimi.it

Margherita Vacchini
margherita.vacchini@unimi.it

[1] Department of Chemistry, Università Degli Studi Di Milano, Via Golgi 19, 20133 Milan, Italy

Published online: 13 March 2025

commensurately modulated by static, wave-like patterns along the *a* direction. The experimentally observed flat configuration is recovered upon averaging the modulated supercell structure into the standard crystallographic cell.

The case of 1-methyluracil shows that libration effects may produce their own long-range order, which does not conform necessarily to crystallographic symmetry. The reason is that libration dynamics cannot be accounted for by colorless symmetry elements, as angular momenta are pseudovectors and transform according to the group action of colored symmetries. This creates the (apparent) discrepancy between average and libration-modulated structures of 1-methyluracil. In the 1970s, Kołakowski introduced the concept of *dynamic symmetry* to describe transformations of quantities associated to axial vectors, like rotational momenta, whose symmetry has two-color operations [13–15]. An X-ray investigation of ethylidene-N,N-diacetamide ($P2_1/c$, CCDC EDACTM10) [14, 16] evidenced sharp and weak off-lattice diffraction spots at reciprocal coordinates ($h0l$, l = odd), not compatible with systematic extinction rules of the *c* glide plane. Kołakowski attributed such features to a modulated distortion of the crystallographic structure, due to correlated librations. He found that the distorted lattice could be described as $P2_1$; however, the corresponding momenta comply to the transformation rules of the colored (Shubnikov) space group $P2_1/c'$, where the apostrophe indicates that the glide representative is augmented with the time reversal operator. Kołakowski proposed to use Shubnikov groups, which are largely employed in materials science to account for magnetic arrangements [17, 18] to describe the dynamic structure of ethylidene-N,N-diacetamide.

The idea that modulated structures could be described in terms of distortions of ideal crystal lattices traces back to the 1960s, when de Wolff and co-workers first discovered incommensurate structure modulations in γ–Na_2CO_3 [19, 20]. As more and more cases of modulated structures were discovered, de Wolff proposed to interpret off-lattice satellite reflections as projections from higher dimensional fully periodic structures [21, 22]. This superspace approach was eventually formalized in the next decade by de Wolff, Janner and Janssen [23, 24], and it is still used nowadays to describe structural modulations in space and in time, especially in the context of magnetic structures, incommensurately modulated crystals and composite lattices [25–27]. Far from being limited to incommensurate distortions, these concepts enable the description of any periodic modulation, including commensurate ones, and those accounting for the transformation rules of axial vectors associated with dynamic symmetries. Thus, the superspace approach provides alternative tools, equivalent to those exploited by colored groups, to interpret structured lattice distortions in terms of high-order symmetries.

We stress that breaking of colorless symmetry is different from disorder, which manifests as random deviations from the idealized crystal structure, either in the whole bulk lattice or along specific directions and planes. In this contribution, we recover Kołakowski's concept of dynamical symmetry with the aim of understanding correlations between structural and dynamic degrees of freedom in molecular crystals. We chose acrylic acid (CCDC ACRLAC02) [28] as a suitable test bench for our proof of concept. We demonstrate that periodic lattice distortions, not appreciable if one looks at the average crystallographic structure, originate from a low-frequency phonon instability at the Γ point of the first Brillouin zone. These distortions are consistent with antiferromagnetic I_cbam (or $C_1m'm'm$) symmetry and may play a role in triggering the transition to the high-density polymorph of acrylic acid at high pressure. Hints to look for such effects in real X-ray diffraction experiments are suggested.

Methods

Structure selection

The crystal structure of acrylic acid ($C_3H_4O_2$, MW 72.064 amu, CAS 79–10-7, Fig. 1) was retrieved from the current release of the Cambridge Structural Database (CSD v5.45 update 2, June 2024) [2].

The ACRLAC02 entry [28] at T = 125 K in *Ibam* (nº 72) was selected, as it was the only available at standard pressure with a reasonable (< 5%) *R* factor, without evidence of disorder. Moreover, acrylic acid is small enough to allow

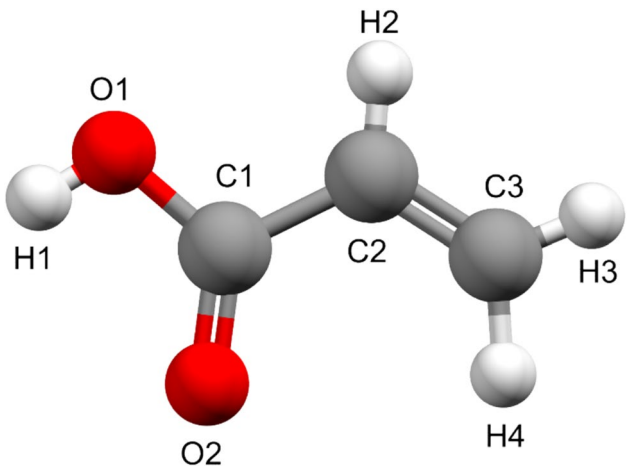

Fig. 1 Structure of acrylic acid. The molecular geometry was retrieved from CSD ACRLAC02 and hydrogen atom positions were renormalized to neutron values according to standard MiCMoS procedures. The atom numbering scheme employed in this work is also shown

both high-grade quantum and classical simulations at a reasonable computational cost. The other crystal structures of acrylic acid belong to the high-*p* $P2_1/c$ form, which is stable above 0.65 GPa [29, 30].

Quantum simulations

Periodic DFT simulations were carried out with the CRYSTAL17 program [31] to study the phonon spectrum of crystalline acrylic acid. The hybrid PBE0 and B3LYP Hamiltonians were tested, as well as the Minnesota-class HSE06 one, which was augmented with the D3 Grimme's empirical correction for dispersive contributions [32]. Peintinger's pob-TZVP Gaussian basis set [33], specifically optimized for solid-state calculations, was used throughout. Atomic coordinates and cell parameters were fully relaxed at 0 K under the adiabatic approximation to ensure proper evaluation of the potential derivatives. The convergence criteria on the maximum root mean square (RMS) of Hellman–Feynman forces and atomic displacement were set at $3{\cdot}10^{-5}$ and $1.2{\cdot}10^{-4}$ au, that is, one order of magnitude smaller than standard tolerances. As for the electronic SCF calculations, an eigenvalue level shifter of 0.5 hartree was applied to accelerate convergence [34]. The cutoffs for the evaluation of Coulomb and exchange integrals were set to 10^{-8} and 10^{-14}. The normal mode analysis was carried out at Γ point. All quantum simulations produced qualitatively the same results; if not otherwise specified, we here discuss the outcomes from the HSE06-D3 Hamiltonian. Full details of steering parameters of CRYSTAL calculations and relevant results may be found in Supporting Information (SI), Section S1.

Classical molecular dynamics simulations

The MiCMoS v2.3 platform [35, 36] was used to generate a roughly cubic $4\times3\times6$ supercell, with edges ~ 39 Å long, hosting 576 molecules. This model underwent 5×10^5 steps of classical molecular dynamics (MD) simulation with a time step of 2 fs, corresponding to a 1-ns long trajectory. The standard leap-frog integrator was applied in conjunction with the built-in Lennard–Jones-Coulomb (LJC) force field [37] and a Berendsen thermostat with a relaxation time of 0.6 ps was set at $T=125$ K. Two different pressure control algorithms were checked: first, a Berendsen barostat was employed with a compression factor of 0.4 atm, in conjunction with a cutoff of 16 Å for long-range interactions; then, a Parrinello-Rahman anisotropic barostat with coupling strength of 4.0 kg was applied [38] and long-range cutoff increased at 18 Å. Both methods gave similar results. If not otherwise specified, only the Parrinello-Rahman outcomes are discussed in the following. Full information on the algorithm and steering parameters used for the MD calculations can be found in Section S2 SI. The total X-ray scattering output was predicted in the reciprocal lattice planes (*hk*0) and (*h*0*l*) for both the perfect crystal and the MD-thermalized structures (Section S2.2 SI).

Reproducibility

Quantum simulations were carried out with the publicly available commercial CRYSTAL17 software (https://www.crystal.unito.it/). Classical calculations were performed with MiCMoS v2.3 (https://sites.unimi.it/xtal_chem_group/), which can be downloaded free of charge under the specified citation and use conditions. Relevant steering parameters and procedures for both programs are deposited in the Supporting Information (Sections S1–S2 SI). The corresponding output files, including MiCMoS trajectories, can be downloaded freely from the public repository Zenodo (https://doi.org/10.5281/zenodo.14549294). This ensures full reproducibility of all the calculations here described.

Results and discussion

CSD search of *Ibam* structures

An unfiltered survey of the 5.45 release (November 2023) of the CSD reveals that 533 crystals adopt the *Ibam* (or equivalent) symmetry within the full set of 1284316 deposited structures. Filtering through "only organics", "3D coordinates determined", "no errors", "no polymeric" and "no ions", resulted in just 73 entries surviving (0.006%), of which 27 refer to multiple determinations of 1-methyluracil (METURAXX), and 7 to the low-*p* form I of acrylic acid (ACRLACXX). Almost all the molecular *Ibam* structures share the same common packing feature (Fig. 2a), namely a stacking of perfectly planar molecular layers along the [001] direction. The reason is that molecules sit exactly on the (*a*,*b*) mirror plane. This results in a symmetry-constrained arrangement of infinite parallel sheets, which extend along the *a* and *b* directions because of the perpendicular glide operators. This motif is typically adopted by flat molecules with an intrinsic mirror element, like purine derivatives (PYZPYT01) or pentadienoic acid (BASBON), but it is compatible also with compounds with an intrinsic three-dimensional structure (MIGBIQ, QOQSIY). In this case, at least one mirror-symmetric conformer must exist, whose molecular *m* operator can be made coincident with the corresponding point element of the *Ibam* group. The only exceptions are boronic acid derivatives NIQZAP and NIQZET, which do not sit on the mirror plane but weave a "X" motif of tail-to-tail hydrogen-bonded dimers along the [1 1 0] and [1 $\bar{1}$ 0] face diagonals.

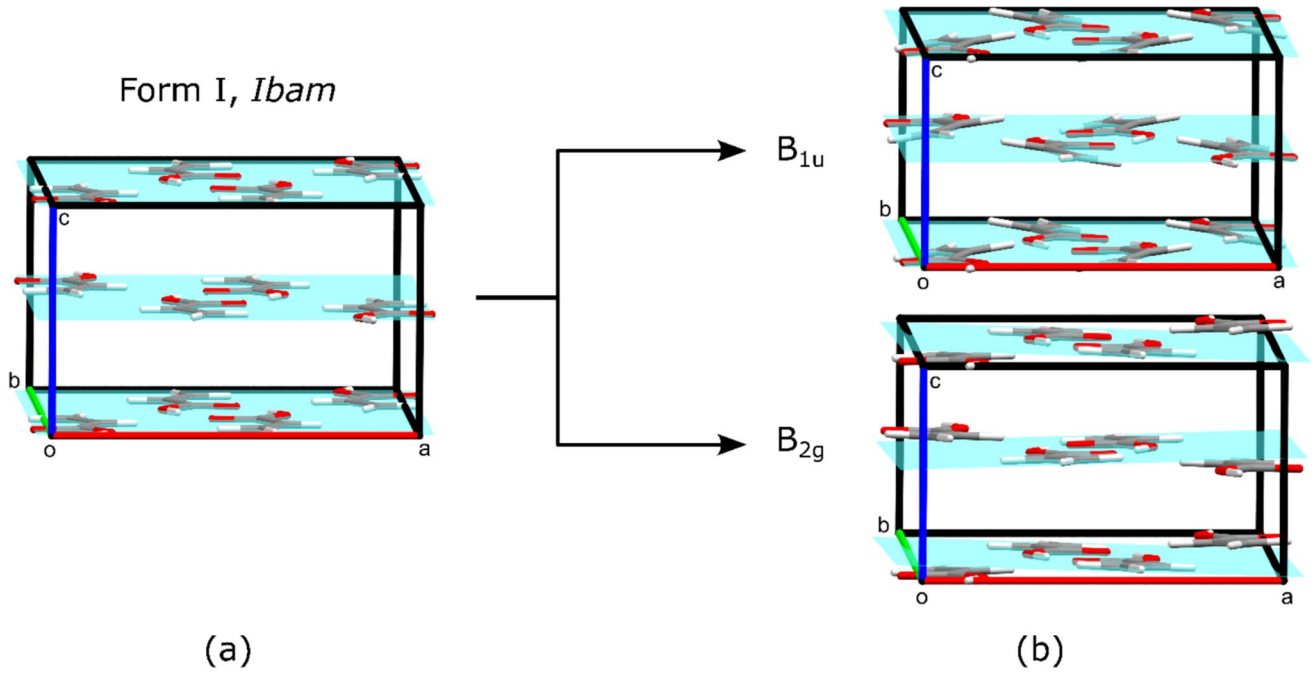

Fig. 2 **a** Experimental crystal packing of acrylic acid (form I, *Ibam*) at $T = 125$ K. **b** Deformation of the molecules in cell upon application of atomic displacements along the B_{1u} and B_{2g} normal modes with imaginary frequency. The least squares planes passing through the dimers are also shown, which for the B_{1u} mode correspond exactly with the (002) crystallographic family. A scale factor of ~ 2 is applied to all the coordinate displacements to enhance the distortions

Crystal packing of acrylic acid

Here, we focus on form I of acrylic acid at low pressure (ACRLAC02, Fig. 2a) [28]. The molecules are associated in pairs held together by cyclic hydrogen bonds. This recognition mode is common in carboxylic acids with low molecular weight [39–41]. The hydrogen bonded dimers form flat layers parallel to the (*a*,*b*) plane, stacked along the [001] direction. Adjacent layers are displaced by ~ 7.7 Å along the [110] face diagonal and are separated by a vertical distance of ~ 3.1 Å. The *c* axis corresponds to roughly two interlayer separations (6.206(2), experimental; 6.430(6) Å, MD) and is 0.4–0.6 Å shorter than 4 van der Waals radii of carbon (1.7 Å) [42]. Thus, two layers are accommodated per unit cell.

Periodic DFT optimization and normal mode analysis

The unit cell of acrylic acid was fully relaxed under the symmetry constraints of the *Ibam* space group at various DFT levels of theory (see "Methods"). The predicted length for the *c* cell axis is invariably shorter than both experimental and MD estimates (6.059 Å, PBE0; 6.117 Å, B3LYP; 5.485 Å, HSE06 + D3). This is due to the thermal shrinking of the whole lattice, as DFT predictions refer to the static structure at 0 K. The driving force is provided by attractive van der Waals interactions, as it can be appreciated by the dramatic (~ 1 Å) reduction of the *c* edge length when dispersions are explicitly added to the Hamiltonian through the Grimme functional [43]. The net outcome is that stacked layers of molecules along *c* are significantly closer in the DFT-optimized structures.

Figure 2b shows the relevant results of the normal mode analysis (see also Tables S6-S7 SI and Figure S1 SI). Two modes having B_{1u} and B_{2g} symmetry with large imaginary frequency are invariably found at the Γ point. A third imaginary mode, with symmetry A_u, is found only by the HSE06 + D3 Hamiltonian. The latter is associated to a small hessian eigenvalue, whose sign depends critically on the level of theory adopted (Table S6 SI). On the contrary, the imaginary modes B_{1u} and B_{2g} are consistently found also with other Hamiltonians (Section S1 SI), indicating that they reflect the intrinsic and genuine dynamic features of the title compound. They correspond to low-energy, high-amplitude librational distortions of the asymmetric unit. These librations are associated to Hessian eigenvectors with negative eigenvalues, meaning that the *Ibam* crystal structure sits on a saddle point of the potential energy hypersurface. Any displacement along such normal coordinates is expected to lower the energy of the crystal at the expense of breaking the (colorless) symmetry.

MD simulations

Finite temperature effects were included by classical molecular dynamics (MD) simulations, which reproduce quantitatively the experimental cell parameters at 125 K (Table S11 SI). The maximum and average absolute errors on cells edges read + 3.61% and 1.97%, in line with the expected accuracy of the force field and the algorithm [44]. Deviations of predicted cell angles from 90° do not exceed 0.3°, which is below the 2σ limit of the simulation. The predicted density (1.301(2) $g{\cdot}cm^{-3}$) also compares well with the experimental one (1.317 $g{\cdot}cm^{-3}$). Accordingly, the residual rotational correlation, as estimated from the C3-C5 interatomic vector (Fig. 1), is stable at ~ 99% (Figure S2 SI) throughout the whole trajectory, indicating that the structure remains perfectly crystalline. The mean-squared displacement (MSD) of molecular centers of mass (Figure S3 SI) quickly increases to a limit value of 3.25(1) $Å^2$, which remains constant over the 100–1000-ps range. This means that the MD-predicted structure is partly distorted with respect to the pristine lattice, with ~ 1.8 Å large molecular displacements from the expected crystallographic positions. The nature of the distortion is evident from direct inspection of the trajectory. Figure 3a, b shows the time-averaged simulation box and the space–time averaged unit cell from the last 200 ps of the simulation. The *Ibam* flat arrangement of molecular sheets in the (*a*,*b*) plane is broken into static periodic oscillations along the [100] direction, with wavelength comparable to the length of the *a* cell axis (9.952(2), experimental; 9.761(13) Å, MD). The flat conformation of individual molecules is mostly preserved, but adjacent dimers along *a* are tilted with respect to one another. Two typical deformation patterns are clearly recognizable by looking along the [010] direction. The most frequent one produces waves, consistent with the libration associated with the strongest B_{1u} imaginary mode (Figs. 2 and 3).

The amplitude of the oscillations is quite small and is consistent with a ~ 0.5 Å large deviation from the planarity of the whole sheet, which corresponds to a tilt angle of ~ 14°, computed as the dihedral between the main molecular plane (C3-C4-C5, Fig. 1) and the plane containing the whole sheet. The other pattern appears whenever rows of dimers running along *b* are periodically arranged at two different heights in the [100] direction (Fig. 3), giving rise to a sort of repeated step pattern. This stepwise deformation mode occurs randomly along *c* and is consistent with the second most negative B_{2g} imaginary mode (Fig. 2b). In any case, the B_{2g} modulation has the same periodicity as the B_{1u} one discussed above. Also, the oscillations have roughly the same magnitude, with maximum height of the "step" of ~ 0.4 Å. Finally, a feature common to both the wave- and step-like modes is a slight displacement of neighboring layers with

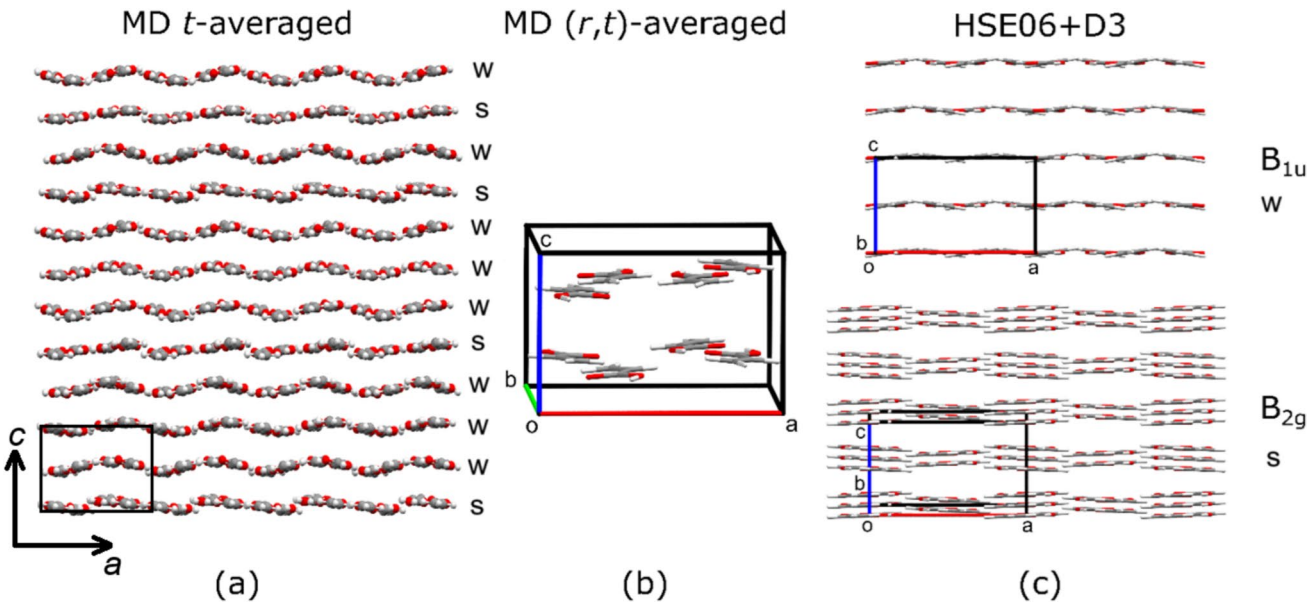

Fig. 3 **a** Time-averaged simulation box over the last 200 ps of the trajectory viewed down the *b* axis. The black box represents one crystallographic unit cell. Subsequent layers along c are labelled as "*w*" or "*s*" depending on whether they are "wave-like" or "step-like" (see text). **b** Same as (**a**), after that translation-related molecules are further averaged into one crystallographic unit cell (atom coordinates in Table S15 SI). Molecules are almost flat, but residual modulation is still appreciable. Only the majority wave-like motifs were included in the average. The translation of [0.25 0 0.25] is due to a different choice of origin and has no physical significance. **c** Patterns generated by the B_{1u} and B_{2g} imaginary modes on the asymmetric unit in *Ibam* symmetry, associated with the wave-like (*w*) and step-like (*s*) motifs. The coordinate displacements were enhanced by a factor ~ 2 to make them appreciable. The picture of the B_{2g} mode is slightly tilted with respect to the [010] projection to make visible the step pattern along *a* formed by adjacent dimers

respect to one another. This is consistent with lacking strong directional forces along the *c* direction.

MD outcomes are worth of note for the following reasons. First, neither structural nor symmetry constraints were applied during either the simulations or the post-processing stage, indicating that the lattice distortion develops spontaneously within 50–100 ps. Likely, this effect is triggered by the tendency of neighboring layers to alleviate the steric hindrance between molecules in van der Waals contact. Second, and most important, MD-predicted modulations agree with structural distortions suggested by DFT quantum simulations along the imaginary vibration modes (compare Figs. 2 and 3). This result reassures us of the correctness of the force field in catching the correct dynamics of the crystal. The true ground state of acrylic acid is commensurately distorted, and these modulations should be integrated into any sensible structural model for this system. Noteworthy, when the time-averaged simulation box is further shrunk back into one crystallographic unit cell, oscillations cancel out almost completely (Fig. 3b). Some residual deviations from planarity are still appreciable in the MD-averaged cell, with main molecular planes not exceeding 5° of tilting. We attribute such residual deviations to a slight error of the classical MD force field in predicting the correct phases of the oscillations, and to the limited size of the simulation box that cannot guarantee a complete sampling (see also the discussion below). However, the underlying picture is qualitatively accurate and strongly suggests that structural modulations cannot be longer appreciated once that a spacetime average model of the lattice is produced by standard X-ray methods.

Predicted scattering intensities and violation of systematic extinctions

The effect of the modulations described in Fig. 3 can be inferred from the inspection of the reciprocal lattice. For this purpose, in the absence of available experimental diffraction images, the scattering intensities of the perfect *Ibam* lattice and the MD-evolved one were calculated and compared (for more details, see Section S2.2 SI). Figure 4 shows the computationally predicted scattering intensity in the (h0l) and (hk0) planes, as reconstructed by atomic scattering summations over the whole simulation box. Due to the finite size of the simulation box, some artifacts in the form of shashlik-like patterns are also present and are particularly evident both close to the origin and some first order reflections, like

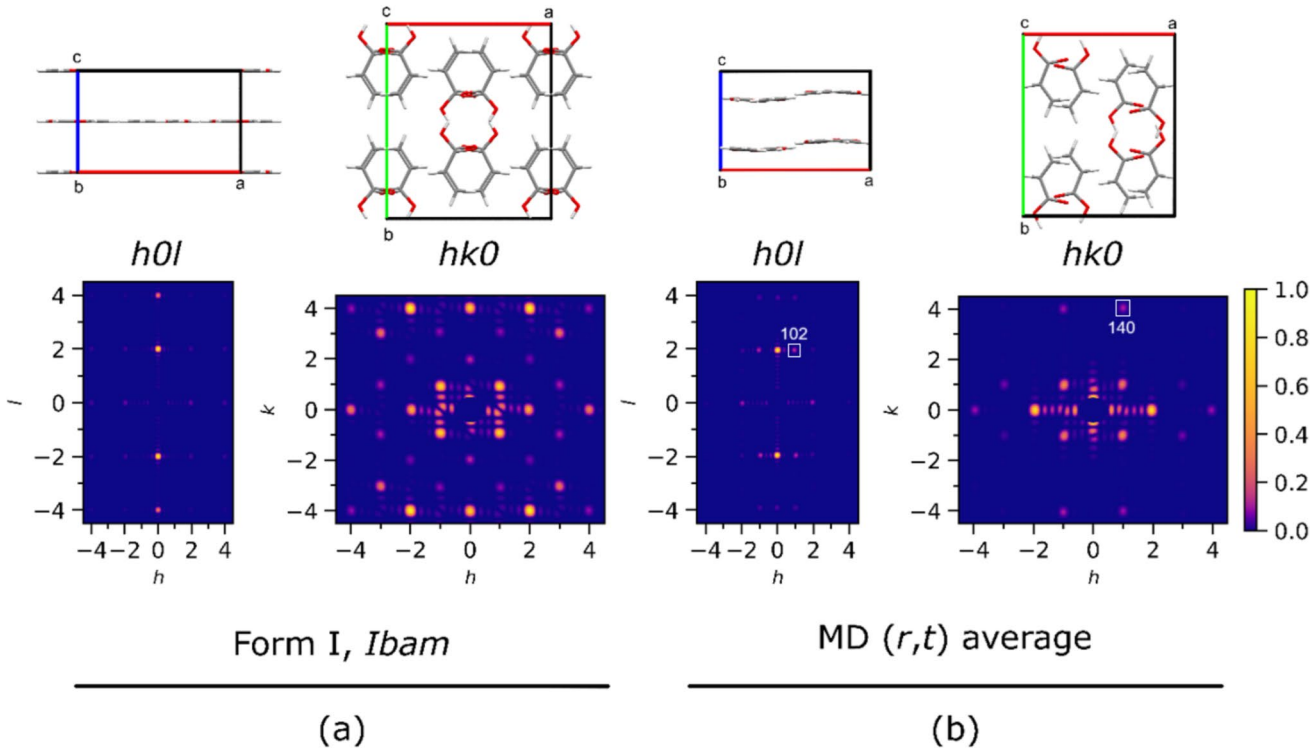

Fig. 4 **a** Predicted scattering intensities in the (h0l) and (hk0) planes around the origin of the reciprocal lattice of the perfect acrylic acid crystal in *Ibam*. The shashlik-like intensity patterns along the reciprocal axes in the vicinity of the origin are an artefact due to the finite dimensions of the simulation box. **b** Same as (**a**), upon averaging the predicted scattering intensity from the last 200 ps of the trajectory. Some intensities are softened due to thermal motion, but (140) and (102) reflections appear, which violate the systematic extinction rules for *Ibam* (see text)

(100) and (010). The outcome from the perfect *Ibam* lattice (Fig. 4a) is compared with the MD-evolved one in the last 200 ps of the trajectory (Fig. 4b). Reflections (140) and (102) are extinct in the *Ibam* structure due to the combined effect of glide planes and Bravais centering (Table S13 SI). In contrast, intensities at (140) and (102) are clearly nonzero after MD thermalization, indicating that the lack of the *m* operator produces the loss of a whole coset of elements. The MD space–time averaged structure belongs to *P*1, since symmetries are not included in the structural model, apart from the translation, which is implicitly accounted for by the supercell approach. If the *P*1 average structure is analyzed by the ADDSYM routine of PLATON [45], a $P2_1/c$ alternative is suggested (Table S14 SI). Accordingly, the MD-predicted nonzero Bragg reflections (Fig. 4b) are consistent with the systematic extinctions of this latter space group. An interpretation is that the action of either the B_{1u} or B_{2g} imaginary modes (Fig. 2) destroys the C_2 symmetry along [001], inducing the lowering of the point group from *mmm* to 2/*m*.

Intriguingly, the high-*p* phase of acrylic acid bears hydrogen-bonded dimers which are no longer constrained in flat sheets, and whose symmetry can be described as $P2_1/c$ as well [29, 30]. Similar wave-like motifs also develop in this phase (Figure S6a SI). Figure S6b SI shows the geometric superposition of one representative layer of our MD-averaged structure and the high-pressure form II ACRLAC04 [29]. Noteworthy, the molecular orientations in the distorted low-*p* lattice are like those in the high-*p* phase, suggesting that the wave-like deformation is not an effect of the phase transition. The main difference between forms I and II is that adjacent layers are mutually shifted, as can be appreciated by comparing the corresponding stacking features along [001] (Figure S5 SI). It is tempting to say that the dynamic perturbation of the orthorhombic form I into a $P2_1/c$ modulation might help to initiate the phase transition at higher *p*. However, deviations from the *Ibam* symmetry at room pressure are small (Figs. 2 and 3) and they could be even exaggerated by our force field–based procedure. The reason is that small displacements of neighboring molecular layers along *c* are probably already present in the low-*p* crystal, as (001) is the main slip plane (Figure S7 SI). Any slipping defect would imply random phase changes of the modulations in the [100] direction. When it comes to our classical simulations, these defects are unavoidably amplified and may come uncompensated due to the small space–time scale of the model ($\sim 4^3$ nm^3 for 1 ns). Overall, the net outcome is that the exceptions to systematic extinction rules shown in Fig. 4 are overestimated. If they were truly present in real diffraction images, their intensities would likely be very low. Moreover, we have no explicit evidence that the monoclinic cell is the best choice to account for the predicted modulations, as different force fields might suggest different selections of surviving symmetry elements. We cautiously consider these outcomes as a warning and a call to carefully explore the reciprocal lattice in search of deviations from the systematic extinction laws, since such deviations, even if very weak, may offer valuable insights into the real structure and dynamics of the crystal.

Colored symmetries and superspace groups

Kołakowski's concept of dynamic symmetry provides a consistent and robust framework to interpret the distortions predicted in the title compound. The idea is that deformations of the pristine lattice emerge according to colored symmetry operations, which apply to dynamic elements of the crystal. In turn, a *dynamic element* is the smallest symmetry-independent structural unit, which bears the same susceptibility to the action of librational forces [13]. In acrylic acid, the dynamic element is the hydrogen-bonded dimer, as tightly bound pairs of molecules experience the most correlated motion. Libration modes produce a (partial) out-of-plane rotation of the dimers. Their dynamics is described by the corresponding angular momenta, which are axial vectors; colorless crystallographic symmetries are insufficient to describe the full set of transformations of axial vectors. This is the reason why the modulated (static) structure loses the mirror plane and—likely—two out of three C_2 axes (see above). Colorless operations cannot account, for example, for the sign reversal of axial vectors upon reflection. This is possible only by including the time reversal operator, which leads to the extension of the 230 colorless space groups to the 1651 (grey + colored) Shubnikov groups [17, 46]. Alternatively, superspace symmetry can be exploited [23, 27]. In this framework, a crystal lattice described by (3 + 1) superspace symmetries accounts for both modulation and action of the time-reversal operator.

Figure 5 shows a scheme of the idealized dynamic structure of acrylic acid. Dimers are condensed to spheres drawn at their center of mass. The spheres are colored red (black) if the displacement occurs above (below) the (*a*,*b*) plane. Stacked planes at $z = 0$ and $z = ½$ along [001] adopt a checkerboard pattern of deformations that alternate above or below the plane, irrespective of the normal coordinate (B_{1u} or B_{2g}) to which they refer (Fig. 5b). Overall, the motif is consistent with a [½ ½ 0] modulation of the time inversion operator, which generates a type IV $I_c bam$ unit cell (n° 72.546) according to the Belov-Neronova-Smirnova (BNS) notation [47]. The same group is referred to as $C_I m'm'm$ (n° 65.19.563) according to the Opechowski-Guccione (OG) notation [48], which is also used in the Litvin's tables [46] of magnetic space groups (Fig. 5a). Moreover, the combination of a one-period commensurate modulation along the *c*-axis and time reversal is consistent with symmetry of the 72.7 $Imcb(00\gamma)0s0$ (3 + 1)

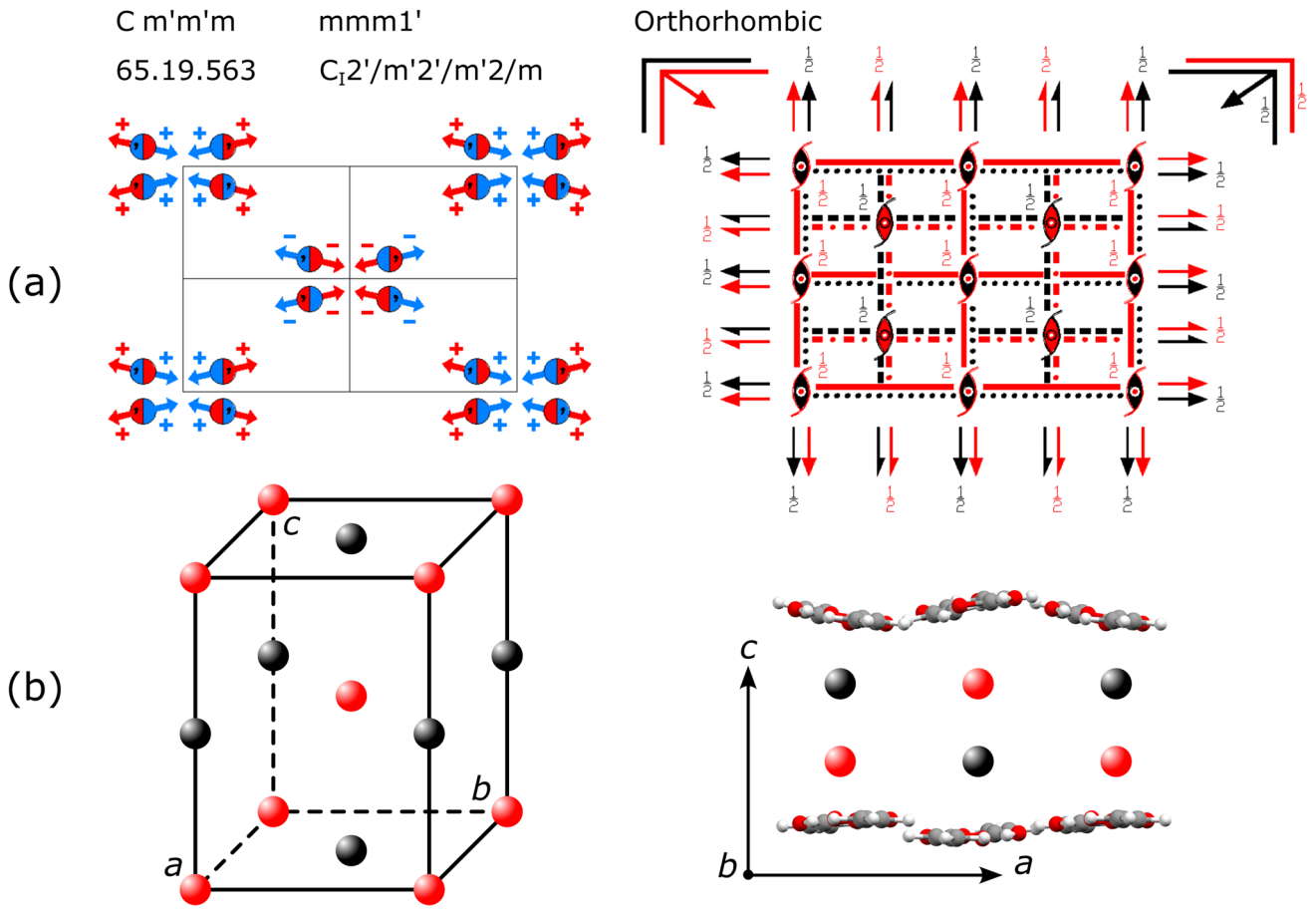

Fig. 5 **a** Symmetry operators of the $C_Im'm'm$ group, corresponding to I_cbam according to the BNS notation, taken from the Litvin's table of Shubnikov groups [46]. Operators augmented with time inversion are written in red. **b** Scheme of dynamic symmetry in acrylic acid. Spheres correspond to the center of mass of dimers, and colors indicate whether the dimer is displaced above (red) or below (black) the (*a*,*b*) plane. Molecular motifs along the [100] direction, taken from the time-averaged MD simulation box and seen along *b*, are shown on the right for the sake of comparison

D superspace group [25], where *Imcb* is an equivalent axis setting, 00γ is the modulation vector with $\gamma = 1$, and the notation $0s0$ indicates that time reversal is applied alongside the *mcb* generators. This can be easily verified in the transformed cell reference system, as shown in Figure S8 SI.

A key point is that this symmetry, regardless of the space group label, is consistent with an antisymmetric arrangement of the angular momenta, in what is the mechanical analogue of an antiferromagnetic material. This guarantees that the net rotation moment of the unit cell is exactly zero. In other words, the ensemble of dynamic elements of the crystal is consistent with a symmetry that avoids the development of a net rotational momentum in the unit cell. It would be interesting to check whether and to what extent such a condition is satisfied in crystals that can be mechanically activated, with possible implications in the current research and engineering of solid-state energy transducers [49].

Conclusions

In this work, we analyze for the first time the solid-state dynamics of form I of acrylic acid at 125 K from first principles. The structure belongs to the very uncommon *Ibam* space group, where molecules are constrained by symmetry to form completely flat layers of hydrogen-bonded dimers. The nuclear wavefunctions were evaluated in the crystal at the DFT level of theory in the framework of the adiabatic approximation, determining the corresponding normal modes at the Γ point of the first Brillouin zone. Two strong imaginary modes are invariably found, which imply an out-of-plane librational distortion of hydrogen-bonded dimers and produce a commensurate static modulation of the crystal structure, undetected by standard X-ray methods. This distortion is confirmed qualitatively by molecular dynamics simulations, which predict a possible reduction in the colorless crystallographic symmetry that could be detected in real life by a careful inspection

of the systematic extinction rules. However, the lattice can still be dynamically described with the two-color symmetry $I_c bam$ or with the (3 + 1)D $Imcb(00\gamma)0s0$ superspace group, where the time inversion operator produces an antisymmetric arrangement of libration momenta, in what is the dynamical analogue of an antiferromagnetic structure. The net rotational momentum in the unit cell is zero, as it should be for a system in mechanical equilibrium.

One might wonder whether an apparent flat packing in highly symmetric crystals is truly flat. The truth is that the seemingly perfect colorless mirror symmetry in *Ibam* disguises the occurrence of small commensurate distortions, whose physical origin must be traced back to an intrinsic instability of the phonon structure at the Γ point. Probably, the resulting crystallographic structure modulation can be framed in the broader phenomenology of spontaneous symmetry breaking events, which include for example the puckering of organic molecules due to the pseudo-Jahn–Teller effect or the self-assembling of polar nanoregions in ferroelectric relaxors [50, 51]. From a crystallographic viewpoint, such distortions can be interpreted as small perturbations of the perfect *Ibam* structure and may be easily overlooked if dynamic effects are not explicitly accounted for. In this work, we show that librational modulations can be described in terms of dynamic symmetry, where the extension to color group symmetry allows to go beyond the classical, static description of crystal packing.

Supplementary Information The online version contains supplementary material available at https://doi.org/10.1007/s11224-025-02483-w.

Acknowledgements The Authors wish to thank prof. Angelo Gavezzotti for continuous inspiration and encouragement.

Author contributions L. S.: Formal analysis, validation, visualization, writing: review and editing. G. M.: Formal analysis, validation, visualization, writing: review and editing. M. V.: Formal analysis, validation, visualization, writing: review and editing. L. L. P.: Conceptualization, investigation, software, supervision, funding acquisition, writing: original draft.

Funding Open access funding provided by Università degli Studi di Milano within the CRUI-CARE Agreement. Università degli Studi di Milano is acknowledged for funding this work through the Research Support Plan (Piano di Sostegno alla Ricerca) 2023, grant number PSR2023_DIP_005_PI_LLOPR.

Data availability Relevant steering parameters and procedures for computer simulations described in this paper are deposited in the Supporting Information. Molecular dynamics trajectories and outputs of quantum chemical simulations can be downloaded freely from the public repository Zenodo (https://doi.org/10.5281/zenodo.14549295).

Declarations

Competing interests The authors declare no competing interests.

Open Access This article is licensed under a Creative Commons Attribution 4.0 International License, which permits use, sharing, adaptation, distribution and reproduction in any medium or format, as long as you give appropriate credit to the original author(s) and the source, provide a link to the Creative Commons licence, and indicate if changes were made. The images or other third party material in this article are included in the article's Creative Commons licence, unless indicated otherwise in a credit line to the material. If material is not included in the article's Creative Commons licence and your intended use is not permitted by statutory regulation or exceeds the permitted use, you will need to obtain permission directly from the copyright holder. To view a copy of this licence, visit http://creativecommons.org/licenses/by/4.0/.

References

1. Wondratschek H, Müller U (eds) (2004) International tables for crystallography, Volume A1. Symmetry Relations between Space Groups. Published for the International Union of Crystallography by Kluwer Academic Publishers. Dordrecht, Boston, London
2. Groom CR, Allen FH (2014) The Cambridge structural database in retrospect and prospect. Angew Chem Int Ed 53(3):662–671
3. Graulis S, Chateigner D, Downs RT, Yokochi AFT, Quirós M, Lutterotti L, Manakova E, Butkus J, Moeck P, Le Bail A (2009) Crystallography open database – an open-access collection of crystal structures. J Appl Crystallogr 42(4):726–729
4. Wilson CC (2009) A basic introduction to thermal motions of atoms in crystal structures, the underlying potentials and the physical information available from their analysis. Crystallogr Rev 15(1):3–56
5. Gavezzotti A (2022) Dynamic simulation of orientational disorder in organic crystals: methyl groups, trifluoro methyl groups and whole molecules. Acta Crystallogr Sect B Struct Sci Cryst Eng Mater 78(3):333–343
6. Gavezzotti A, Rizzato S, Lo Presti L (2018) The TACO puzzle: a phase-transition mystery revisited. Crystal Growth Des 18(11):7219–7227
7. Gavezzotti A, Lo Presti L, Rizzato S (2022) Molecular dynamics simulation of organic materials: structure, potentials and the MiCMoS computer platform. CrystEngComm 24(5):922–930
8. Macetti G, Sironi L, Lo Presti L (2024) Classical Molecular dynamics simulation of molecular crystals and materials: old lessons and new perspectives in Yanez, M. & Boyd, R. J. (eds.), Comprehensive Computational Chemistry 3:777–803
9. Schomaker V, Trueblood KN (1968) On the rigid-body motion of molecules in crystals. Acta Crystallogr. Sect B Struct Sci Cryst Eng Mater 24:63–76
10. Willis BTM, Pryor AW (1975) Thermal vibrations in crystallography. Published by Cambridge University Press, New York
11. Lo Presti L, Orlando AM, Loconte L, Destro R, Ortoleva E, Soave R, Gatti C (2014) Single N-C bond becomes shorter than a formally double N═C bond in a thiazete-1,1-dioxide crystal: an experimental and theoretical study of strong crystal field effects. Cryst Growth Des 14(9):4418–4429
12. Destro R, Roversi P, Barzaghi M, Lo Presti L (2021) Anharmonic thermal motion modelling in the experimental XRD charge density determination of 1-methyluracil at T = 23 K. Molecules 26:3075
13. Kołakowski B (1977) The 230 or 1651 space groups? Acta Phys Pol, A 52:635–640
14. Kołakowski B (1978) The dynamic symmetry and its application for interpretation of X-ray diffraction patterns. Solid State Commun 25:941–944

15. Kołakowski B (1979) The dynamic symmetry and plastic deformation of diamond lattice. Appl Phys 20:305–312
16. Kołakowski B (1969) The crystal structure of ethylidene-N, N-diacetamide. Acta Crystallogr. Sect B: Struct Crystallogr Cryst Chem 25:1669–1671
17. Lifshitz R (2005) Magnetic point groups and space groups. In: Bassani F, Liedl GL, Wyder, P (eds) Encyclopedia of Condensed Matter Physics. Elsevier, pp 219–226. https://doi.org/10.1016/B0-12-369401-9/00748-8
18. Rodriguez-Carvajal J, Bourée F (2012) Symmetry and magnetic structures. EPJ Web Conf 22:00010
19. Brouns E, Visser JW, de Wolff PM (1964) An anomaly in the crystal structure if Na2CO3. Acta Crystallogr 17:614
20. de Wolff PM, van Aalst W (1972) The four-dimensional space group of Na2CO3. Acta Crystallogr A 28:S111
21. de Wolff PM (1974) The pseudo-symmetry of modulated crystal structures. Acta Crystallogr A 30:777–785
22. de Wolff PM (1977) Acta Crystallogr. Symmetry Operations Displacively Modulated Struct A33:493–497
23. Janner J, Janssen T (1977) Symmetry of periodically distorted crystals. Phys Rev B 15:643–658
24. de Wolff PM, Janner J, Janssen T (1981) The superspace groups for incommensurate crystal structures with a one-dimensional modulation. Acta Crystallogr A 37:625–636
25. Janssen T, Janner A, Looijenga-Vos A, de Wolff PM (2004) Chapter 9.8: incommensurate and commensurate modulated structures. In: Prince E (ed) International Tables for Crystallography. Volume C, Mathematical, Physical and Chemical Tables. Published for the International Union of Crystallography by Kluwer Academic Publishers. Dordrecht, Boston, London, pp 907–955
26. van Smaalen S (2012) Incommensurate crystallography. International Union of Crystallography Monographs on crystallography, vol 21. Published by Oxford University Press Inc, New York
27. Janssen T, Janner A (2014) Aperiodic crystals and superspace concepts. Acta Crystallogr B 70:617–651
28. Boese R, Bläser D, Steller I, Latz R, Bäumen A (1999) Redetermination of 2-propenoic acid at 125K. Acta Crystallogr C 55:IUC9900006
29. Ostwald IDH, Urquhart AJ (2011) Polymorphism and polymerisation of acrylic and methacrylic acid at high pressure. CrystEngComm 13:4503–4507
30. Johnston BF, Marshall WG, Parsons S, Urquhart AJ, Oswald DH (2014) Investigation of acrylic acid at high pressure using neutron diffraction. J Phys Chem B 118(14):4044–4051
31. Dovesi R, Erba A, Orlando R, Zicovich-Wilson CM, Civalleri B, Maschio L, Rérat M, Casassa S, Baima J, Salustro S, Kirtman B (2018) Quantum-mechanical condensed matter simulations with CRYSTAL. WIREs Computational Mol Sci 8(4):e1360
32. Grimme S, Antony J, Ehrlich S, Krieg H (2010) A consistent and accurate ab initio parametrization of density functional dispersion correction (DFT-D) for the 94 elements H-Pu. J Chem Phys 132:154104
33. Vilela Oliveira D, Peintinger MF, Laun J, Bredow T (2019) BSSE-correction scheme for consistent gaussian basis sets of double- and triple-zeta valence with polarization quality for solid-state calculations. J Comput Chem 40:2364–2376
34. Dovesi R, Saunders VR, Roetti C, Orlando R, Zicovich-Wilson CM, Pascale F, Civalleri B, Doll K, Harrison NM, Bush IJ, D'Arco Ph, Llunel M, Causà M, Noël Y, Maschio L, Erba A, Rérat M, Casassa S (2017) CRYSTAL17 user's manual. 2017, University of Turin, Turin, Italy. https://www.crystal.unito.it/documentation.html. Accessed 5 Jan 2025
35. Gavezzotti A, Lo Presti L, Rizzato S (2022) Molecular dynamics simulation of organic materials: structure, potentials and the MiCMoS computer platform. CrystEngComm 24:922–930
36. Lo Presti L, Sironi L, Macetti G (2024) MiCMoS v2.3 user's manual. 2024, Università degli Studi di Milano, Milan, Italy. https://sites.unimi.it/xtal_chem_group/images/MiCMoS_package/v2.3_t/MiCMoS_v2.3_User_Manual.pdf. Accessed 5 Jan 2025
37. Gavezzotti A, Lo Presti L, Rizzato S (2020) Mining the Cambridge Database for theoretical chemistry. Mi-LJC: a new set of Lennard-Jones–Coulomb atom–atom potentials for the computer simulation of organic condensed matter. CrystEngComm 22:7350–7360
38. Rizzato S, Gavezzotti A, Lo Presti L (2020) Molecular dynamics simulation of molecular crystals under anisotropic compression: bulk and directional effects in anthracene and paracetamol. Cryst Growth Des 20(11):7421–7428
39. Gavezzotti A, Lo Presti L (2015) A theoretical study of chiral carboxylic acids. Structural and energetic aspects of crystalline and liquid states. Cryst Growth Des 15(8):3792–3803
40. Sironi L, Macetti G, Lo Presti L (2023) Molecular dynamics investigation of benzoic acid in confined spaces. Phys Chem Chem Phys 25:28006–28019
41. Sironi L, Macetti G, Lo Presti L (2024) Nanoscale inhomogeneities in undercooled benzoic acid: a molecular dynamics study. J Mol Liq B414:126141
42. Dunitz JD, Gavezzotti A (1999) Attractions and repulsions in molecular crystals. Acc Chem Res 32(8):677–684
43. Grimme S (2011) Density functional theory with London dispersion corrections. WIREs Comput Mol Sci 1:211–228
44. Gavezzotti A, Lo Presti L (2019) Molecular dynamics simulation of organic crystals: introducing the CLP-dyncry environment. J Appl Crystallogr 52:1253–1263
45. Spek A (2003) L, Single-crystal structure validation with the program PLATON. J Appl Cryst 36:7–11
46. Litvin DB (2008) Tables of crystallographic properties of magnetic space groups. Acta Cryst A64:419–424
47. Belov NV, Neronova NN, Smirnova TS (1957) Shubnikov groups. Sov Phys Crystallogr 2:311–322
48. Opechowski W, Guccione R (1965) Magnetic symmetry. In: Rado GT, Suhl H (eds) Magnetism, vol II A. Academic Press, New York, pp 105–165
49. Naumov P, Karothu DP, Ahmed E, Catalano L, Commins P, Halabi JM, Al-Handawi MB, Li L (2020) The rise of dynamic crystals. J Am Chem Soc 142(31):13256–13272
50. Bersuker IB (2021) Jahn-Teller and Pseudo-Jahn–Teller effects: from particular features to general tools in exploring molecular and solid state properties. Chem Rev 121(3):1463–1512
51. Lo Presti L, Parravicini J, Soave R, Parravicini G, Mauri M, Loconte L, Di Mei F, Falsi L, Tartara L, Binetti S, Agranat AJ, DelRe E (2020) Observation of an exotic lattice structure in the transparent KTa1−*x*Nb*x*O3 perovskite supercrystal. Phys Rev B 102:214110

Publisher's Note Springer Nature remains neutral with regard to jurisdictional claims in published maps and institutional affiliations.